



## Comparison of surface and hydrogel-based protein microchips

D.A. Zubtsov, E.N. Savvateeva, A.Yu. Rubina \*, S.V. Pan'kov,  
E.V. Konovalova, O.V. Moiseeva, V.R. Chechetkin, A.S. Zasedatelev

*Engelhardt Institute of Molecular Biology, Russian Academy of Sciences, Vavilov str., 32, 119991 Moscow, Russia*

Received 19 March 2007

### Abstract

Protein microchips are designed for high-throughput evaluation of the concentrations and activities of various proteins. The rapid advance in microchip technology and a wide variety of existing techniques pose the problem of unified approach to the assessment and comparison of different platforms. Here we compare the characteristics of protein microchips developed for quantitative immunoassay with those of antibodies immobilized on glass surfaces and in hemispherical gel pads. Spotting concentrations of antibodies used for manufacturing of microchips of both types and concentrations of antigen in analyte solution were identical. We compared the efficiency of antibody immobilization, the intensity of fluorescence signals for both direct and sandwich-type immunoassays, and the reaction-diffusion kinetics of the formation of antibody–antigen complexes for surface and gel-based microchips. Our results demonstrate higher capacity and sensitivity for the hydrogel-based protein microchips, while fluorescence saturation kinetics for the two types of microarrays was comparable.

© 2007 Published by Elsevier Inc.

**Keywords:** Surface and hydrogel-based protein microarrays; Quantitative immunoassay; Immobilization efficiency; Fluorescence measurements; Time of signal saturation

Protein microchips with arrays of individual elements containing immobilized molecular probes specific to various target molecules in analyte solution present rapidly developing proteomic technology for different research and practical purposes (for review see, e.g., [1–4]). The most important applications include quantitative immunoassay of disease-associated markers, allergens, and biological toxins with sensitivity comparable to or higher than that of standard immunological methods. Other applications address protein–protein, protein–lipid, and protein–ligand interactions involved in enzymatic reactions. The rapid advance in microchip technology and a variety of techniques developed by different groups require systematic assessment and comparison of different platforms.

Current formats of protein microchips range from matrix microarrays in which the probes are fixed on glass, plastic, or another two-dimensional support, in the form of

$M \times N$  matrix with  $M$  rows and  $N$  columns, to microwells, microspheres, and microfluidic systems. Probe molecules in the elements of matrix microarrays may be immobilized either on a substrate surface or in the gel pads. Here we study how the mode of immobilization affects the characteristics of protein microchips.

Specifically, we compare the efficiency of antibody immobilization, the intensity of fluorescence signals for direct and sandwich-type immunoassays, and the signal saturation kinetics for the protein microchips with antibodies immobilized on flat glass surfaces and within hemispherical gel pads.

The protocol for the manufacturing of surface microchips with the most favorable characteristics was chosen based on a recent review by Kusnezov et al. [4]. For the gel-based microchips, we applied the copolymerization technology described in our earlier publications [5–8]. To achieve maximal uniformity of the comparison, the two types of microchips were manufactured using similar equipment, the signals were measured with the same

\* Corresponding author. Fax: +7 495 135 14 05.

E-mail address: arubina@biochip.ru (A.Yu. Rubina).

59 devices, and spotting concentrations of probes used for  
60 immobilization and concentrations of target molecules in  
61 analyte solution were identical. The uniformity of these  
62 parameters was thoroughly controlled in the course of  
63 the experiments.

64 For our comparative study we chose the antibody  
65 microchips developed for the detection of prostate-specific  
66 antigen (PSA)<sup>1</sup>, a 240-amino-acid-long glycoprotein with  
67 molecular mass about 30 kDa. PSA is a tissue-specific  
68 tumor marker routinely used in clinical practice [9–11]. It  
69 has been approved by the FDA for early diagnostics of  
70 prostate cancer.

71 Our results demonstrate higher immobilization capacity  
72 and stronger fluorescence signals for the hydrogel-based  
73 protein microchips than for the microchips with surface-  
74 immobilized probes at the comparable kinetics of fluores-  
75 cence saturation. Such differences are most likely related  
76 to the much longer interprobe distances in the gel pads  
77 than in the surface chips, the aqueous environment of  
78 immobilized compounds, and the absence of contacts with  
79 hydrophobic surfaces.

## 80 Materials and methods

### 81 Antibodies and analytes

82 PSA was obtained from Khema-Medica (Moscow).  
83 Monoclonal antibodies to PSA were purchased from  
84 CanAg (Sweden); antibodies PSA-30 (molecular mass 150  
85 kDa) were used as immobilized antibodies, while PSA-66  
86 were used as developing antibodies for sandwich immuno-  
87 assay. Cy5 fluorescence dye, monosuccinimide ester,  
88 Sephadex G-25 coarse, and Bind Silane were purchased  
89 from Amersham Pharmacia Biosciences (Piscataway, NJ),  
90 Micro Bio-Spin chromatography columns were from Bio-  
91 Rad Laboratories (Hercules, CA), and glass slides for the  
92 fabrication of microarrays (Corning 2947 Micro Slides;  
93 3 in. by 1 in.) were from Corning Glass Works (Corning,  
94 NY). Other chemical reagents were obtained from com-  
95 mercial suppliers and used without further purification.

96 Throughout this work we used the following buffer solu-  
97 tions: PBS (0.01 M phosphate buffer, pH 7.2, 0.15 M  
98 NaCl), PBST (PBS with 0.1% Tween 20), and blocking  
99 solution PBSP (PBS with 1% polyvinyl alcohol).

### 100 Fabrication of microchips

101 Gel-based microchips with immobilized antibodies  
102 covalently linked to the three-dimensional gel were fabri-  
103 cated by a polymerization-mediated immobilization  
104 method as described in [5,6,8]. Solutions containing gel-  
105 forming monomers and antibodies were transferred to the  
106 wells of a 384-well microtitration plate (Genetix, New Mil-  
107 ton, UK) and spotted onto Bind-Silane-treated glass slides

using a QArray pin robot (Genetix). Polymerization of the  
gel-forming composition was carried out under UV light  
with maximal wavelength of 350 nm, irradiation intensity  
0.06  $\mu\text{W}/\text{cm}^2$  (GTE lamp F15T8/350 BL, Sylvania, Dan-  
vers, MA), for 40 min at 20 °C. Before carrying out on-chip  
immunoassays, biochips were washed in PBST and then  
with distilled water. After that, biochips were treated with  
PBSP for 40 min and washed with distilled water.

Surface antibody microchips were manufactured on  
glass slides treated with 3-(glycidyoxypropyl)triethoxysi-  
lane as described [4] with slight modifications. The slides  
were washed with 100% ethanol, etched overnight by  
immersion in 10% NaOH, cleaned by sonication in the  
same solution for 15 min, rinsed four times in water,  
washed twice in ethanol, and derivatized in a 3-(glycidyl-  
oxypropyl)triethoxysilane (Fluka, Germany) at room tem-  
perature for 3 h. After silanization, epoxysilanized slides  
were washed with toluene and dried with nitrogen. Phos-  
phate buffer (0.015 M, pH 7.2) supplemented with 40% tre-  
halose was used as spotting buffer. The antibodies were  
spotted using the QArray pin robot mentioned above.  
After spotting, the slides were incubated at 4 °C overnight,  
blocked for 40 min at room temperature in PBSP, and  
washed with distilled water.

For both gel-based and surface microchips the volume  
of spotting solution was about 1 nl per spot.

For control purposes each set corresponding to a given  
antibody concentration in spotting solution [Ab] consisted  
of four cells. We used graded twofold increases in concen-  
trations for the neighboring four-cell sets. Specifically, the  
spotting concentrations for the analysis of immobilization  
efficiency ranged consecutively from  $[Ab]_0 = 0.15 \text{ mg/ml}$   
to  $2^4 \times [Ab]_0$ , while the concentrations of antibodies for  
the sandwich-type immunoassays and for the study of  
kinetic curves using direct immunoassays ranged from  
 $[Ab]_0 = 0.1 \text{ mg/ml}$  to  $2^3 \times [Ab]_0$ . Additionally, the gel-based  
microchips also contained four-cell sets with gel pads with-  
out immobilized antibodies. An overview of the microchip  
scheme and the corresponding cells on gel-based and sur-  
face microchips is presented in Fig. 1.

The radii of the cells for both surface and gel-based  
microchips were 75  $\mu\text{m}$ , while the distances between the  
centers of the cells were 250  $\mu\text{m}$ . The reaction chamber  
was covered with a transparent plastic plate. The volume  
of the reaction chamber was about 40  $\mu\text{l}$  (area  $\sim 1 \times 1 \text{ cm}^2$   
and height 400  $\mu\text{m}$ ).

The study of microchips under microscope in transmit-  
ted light revealed distinct slightly oblate hemispherical gel  
pads on gel-based microchips (cf. [5,6]). There were no  
observable three-dimensional features on surface  
microchips.

### Labeling with Cy5 fluorescence dye

To label PSA and antibodies at amino groups, 10  $\mu\text{l}$  of  
Cy5 succinimide ester solution (protein:dye molar ratio  
1:5) in freshly distilled dimethyl sulfoxide was added to

<sup>1</sup> Abbreviations used: PSA, Prostate-specific antigen; PBS, phosphate-buffered saline.

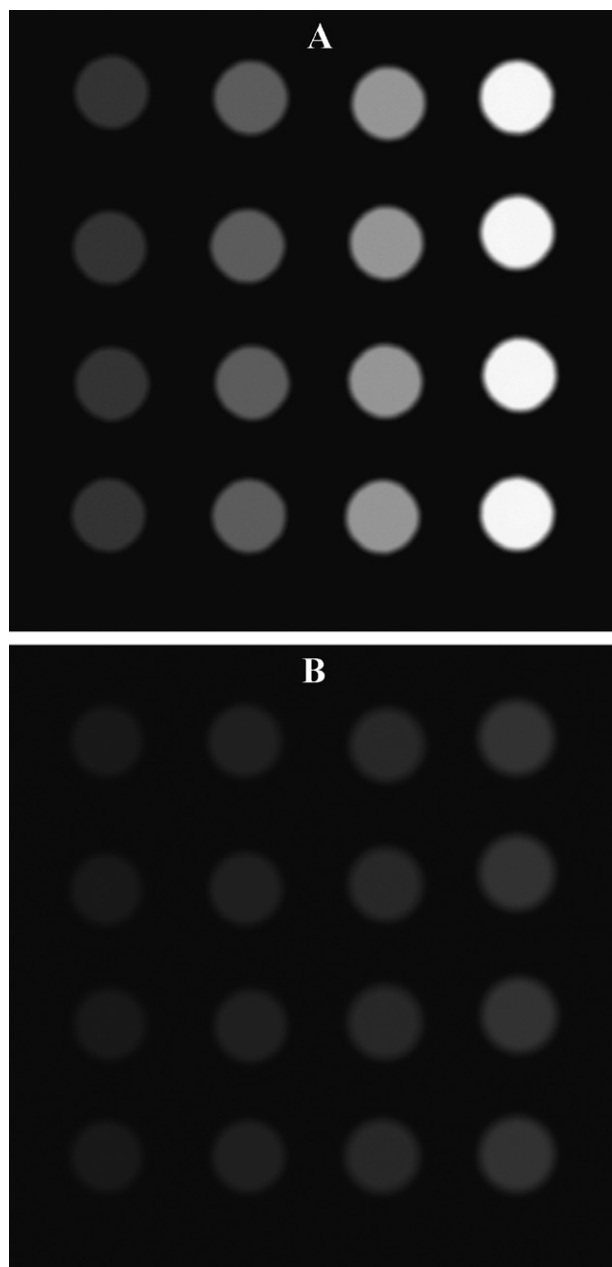


Fig. 1. Counterpart fragments of gel-based (A) and surface (B) microchips with the cells containing immobilized antibodies to PSA in different concentrations after binding with PSA and staining with Cy5-labeled antibodies (sandwich-type immunoassay). The concentrations of antibodies were 0.1, 0.2, 0.4, and 0.8 mg/ml of spotting solution (in columns from left to right, where each column of four elements corresponds to the same concentration of antibodies). Concentration of PSA in analyte solution was 60 ng/ml.

163 100  $\mu$ l of PSA or antibody solution (2–5 mg/ml) in 0.01  
 164 bicarbonate buffer, pH 9.5, and the mixture was stirred  
 165 for 1 h at 20  $^{\circ}$ C. Labeled PSA and antibodies were purified  
 166 on a Micro Bio-Spin column with Sephadex G-25 coarse  
 167 equilibrated with PBS. The protein: Cy5 molar ratio was  
 168 determined by the absorbance at 280 and 650 nm and  
 169 assessed to be about 1.0.

### Microchip imaging and data analysis

170

Quantitative fluorescence measurements were carried  
 out with a custom-built fluorescence microscope equipped  
 with a cooled Charge-coupled device camera, Peltier ther-  
 motable, temperature controller, and a computer with  
 data-acquisition board [12]. The signals from Cy5 dye were  
 obtained using 649/670 nm excitation/emission filters. The  
 exposure time was 1 s. Fluorescence signals from individual  
 cells were processed using ImaGel Research program  
 developed in our laboratory.

To assess the efficiency of immobilization and to mea-  
 sure the results of sandwich-type immunoassays, the chips  
 were washed with water and the resulting fluorescence  
 intensity was calculated using the formula

$$J = \frac{C - B_{d.c.}}{B_{r.g.} - B_{d.c.}}, \quad (1) \quad 185$$

where  $C$  is the median fluorescence calculated for the image area  
 occupied by a probe cell (or median value corresponding to the set  
 of pixels covering image area). To take into account possible spa-  
 tial inhomogeneity of the illumination source, the microchip slide  
 was replaced by a slide of red glass of identical size, and the cor-  
 responding median fluorescence intensity within a position occu-  
 pied by a gel pad,  $B_{r.g.}$ , was measured. This value was corrected  
 by noise signal  $B_{d.c.}$  produced by dark current at zero illumination  
 intensity.

The corresponding fluorescence signals for direct anti-  
 gen–antibody immunoassays during the study of kinetic  
 curves were measured under buffer solution and were cal-  
 culated as

$$J(t) = \frac{C(t) - C(0)}{B_{r.g.} - B_{d.c.}}, \quad (2) \quad 200$$

where  $C(t)$  is the integral fluorescence at moment  $t$  calculated for  
 the image area occupied by a probe cell and  $C(0)$  is the fluores-  
 cence of the same area at the initial moment  $t = 0$ .

### Results

204

All experiments at a given concentration of antibodies in  
 spotting solution (for the assessment of immobilization effi-  
 ciency) and that of antigen in analyte solution (for both  
 sandwich and direct immunoassays) were repeated twice.  
 The lowest signal-to-noise ratio exceeded 2.0, while the rela-  
 tive scattering in experimental data was within 5–10%.  
 The data presented below correspond to the median values  
 for four-cell sets with identical concentration of immobi-  
 lized antibodies (see Materials and methods and Fig. 1).  
 All measurements were performed at 25  $^{\circ}$ C.

### Antibody immobilization efficiency

215

The fraction of immobilized antibodies was assessed by  
 comparing the fluorescence signals produced by Cy5-  
 labeled antibodies after immobilization and washing. The  
 chip was washed with PBST until the fluorescence signals  
 remained constant. The degree of immobilization was

221 calculated as the ratio of the fluorescence signals before  
222 and after washing.

223 Fig. 2 shows the dependence of immobilization effi-  
224 ciency for antibodies to PSA on the surface cells and in  
225 the gel pads on the concentration of antibodies in spotting  
226 solution. As is seen in Fig. 2, in a given range of concentra-  
227 tions the immobilization efficiency in the gel pads remains  
228 approximately constant  $\sim 30\%$  with the enhancement of  
229 antibody concentration in spotting solution. At the same  
230 time, the corresponding efficiency for the surface cells  
231 drops rapidly beginning from concentrations  $[Ab]$   
232  $\geq 2.5$  mg/ml. The possible explanation of such dependenc-  
233 es will be presented below in the Discussion.

#### 234 Sandwich immunoassay

235 As antibody microchips are used primarily for analytical  
236 purposes, we compared the sensitivity of gel-based and sur-  
237 face microchips in a sandwich-type immunoassay com-  
238 monly used for the assessment of antigen concentration.

239 First, 40  $\mu$ l of a solution containing PSA under study  
240 was applied on a chip, and biochips were kept at 25  $^{\circ}$ C  
241 for 17 h. PSA was diluted to desired concentration in PBSP  
242 with 0.15% polyvinylpyrrolidone. After incubation, bio-  
243 chips were washed for 20 min with PBST and then with dis-  
244 tilled water. Second, to display the complexes formed  
245 between immobilized antibodies and PSA, a solution with  
246 Cy5-labeled antibodies against PSA (15  $\mu$ g/ml) was incu-  
247 bated on a chip for 2 h. After subsequent washing with  
248 PBST for 20 min, fluorescent signals were recorded.

249 The resulting calibration curves at different concentra-  
250 tions of antibodies in spotting solution are shown in  
251 Fig. 3. Fluorescence signals obtained using the gel-based  
252 protein microchips turn out to be three- to fivefold higher  
253 than those obtained on the surface chips and cover a  
254 broader dynamical range than the corresponding signals  
255 on the surface microchips. The difference in the fluore-  
256 scence intensities grows with the increase of antibody con-  
257 centration in spotting solution.

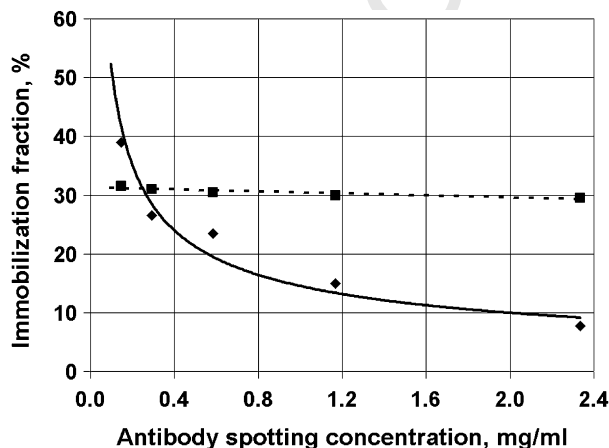


Fig. 2. Dependence of immobilization efficiency for antibodies to PSA on the surface cells (◆) and in the gel pads (■) on the concentration of antibodies in spotting solution. The antibodies were labeled with Cy-5.

#### Direct immunoassay and kinetics of antigen binding

258

259 Kinetic measurements were carried out using direct  
260 immunoassay for Cy5-labeled PSA applied on the micro-  
261 chips containing immobilized antibodies against PSA in  
262 different concentrations (cf. Fig. 1). Fluorescence signals  
263 from each cell were measured every 15 min for 50 h at  
264 the concentration of the antigen in buffer solution equal  
265 to  $[Ag]_{sol} = 750$  ng/ml (or  $2.5 \times 10^{-8}$  M). Note that the con-  
266 centrations of antigen used for direct immunoassay  
267 exceeded one-two orders of magnitude the concentrations  
268 typical for clinical measurements (and that used for sand-  
269 wich type immunoassay above). These high concentrations  
270 of antigen were chosen to accelerate the kinetics of binding  
271 (cf. Eqs. (5) and (6) below) and to improve the visualization  
272 of cells under buffer solution. In additions, these concentra-  
273 tions cover the range  $K_a[Ag]_{sol} \sim 1$ , where  $K_a$  is the associ-  
274 ation constant for binding between immobilized antibodies  
275 and antigen, suitable for the experimental assessment of  
276 association constant (see Discussion).

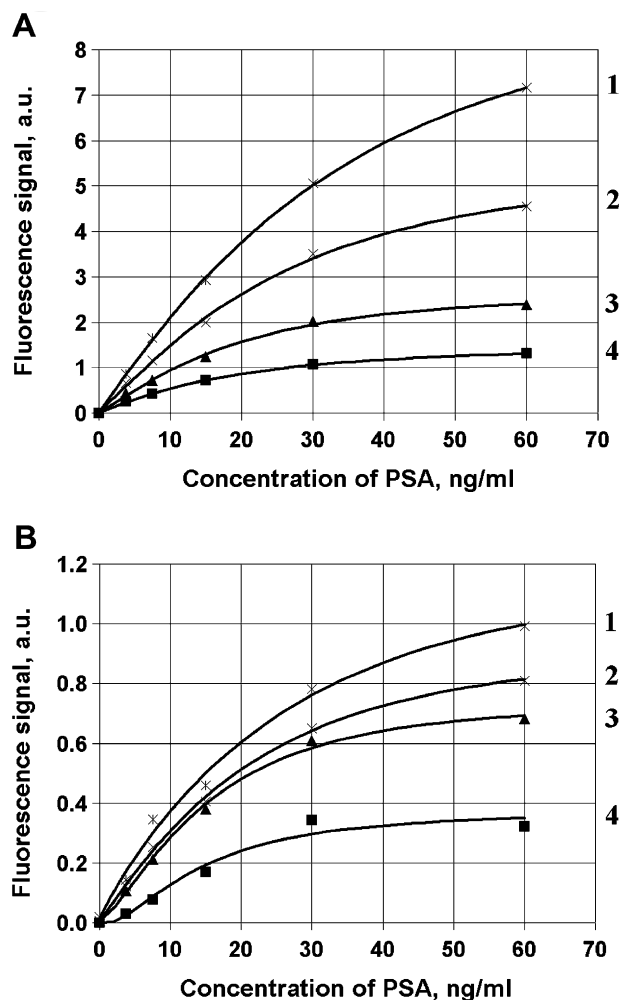


Fig. 3. Calibration curves for sandwich-type immunoassay of PSA obtained with gel-based (A) and surface (B) protein microchips at different concentrations of antibodies in spotting solution: 0.8 mg/ml (1); 0.4 mg/ml (2); 0.2 mg/ml (3); and 0.1 mg/ml (4).



277 The corresponding kinetic curves are shown in Fig. 4.  
 278 The saturation (or binding) time  $\tau_B$  was determined from  
 279 these curves as the time necessary for the fluorescence sig-  
 280 nal to reach 0.9 of the saturation level. Both the signals at  
 281 saturation and those at binding times  $\tau_B$  depend approxi-  
 282 mately linearly on the concentration of antibodies in spot-  
 283 ting solution  $[Ab]$ , which are in this range approximately  
 284 proportional to the number of immobilized antibodies in  
 285 accordance with theoretical predictions (see Figs. 5 and 6  
 286 and Eqs. (3)–(6) below). The linear dependence of satura-  
 287 tion time  $\tau_B$  on  $[Ab]$  shown in Fig. 6 indicates the diffu-  
 288 sion-limited character of binding kinetics (cf. Eqs. (5)–(7)  
 289 in Discussion). The intercepts of straight lines for the  
 290 dependence of saturation time  $\tau_B$  on  $[Ab]$  with y axis cor-  
 291 responding to the limit of low concentration of immobilized  
 292 antibodies  $[Ab]$  provide the approximate estimates for the  
 293 binding times at reaction-limited kinetics.  
 294 We observed about an order of magnitude higher intensi-  
 295 ty of signals at saturation for gel-based microchips com-  
 296 pared to that for surface microchips, while the rates of

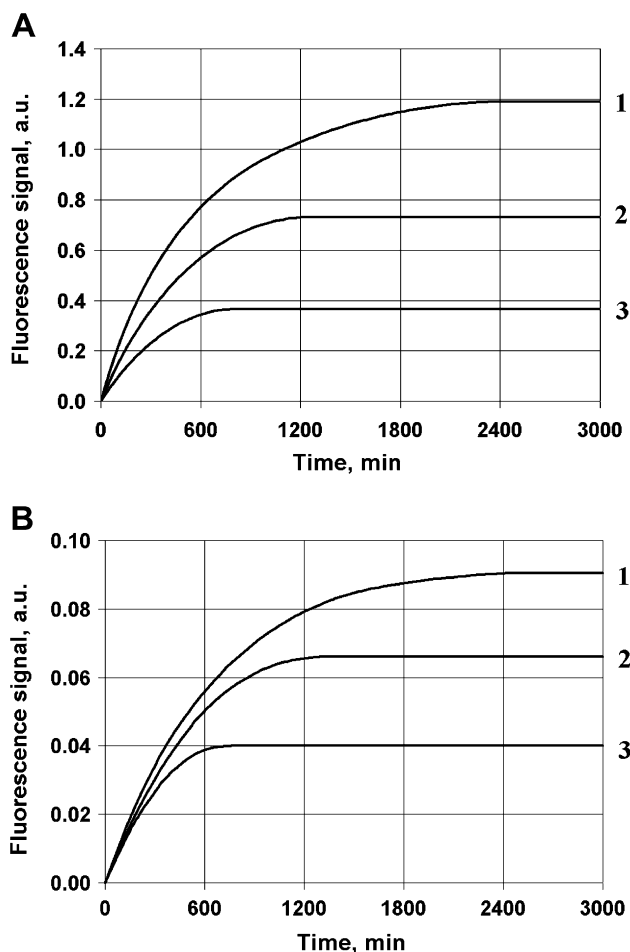


Fig. 4. Kinetic curves for the saturation of fluorescence signals on gel-based (A) and surface (B) protein microchips at different concentrations of antibodies in spotting solution: 0.8 mg/ml (1); 0.4 mg/ml (2); and 0.2 mg/ml (3). The data correspond to direct-type immunoassay with Cy5-labeled PSA.

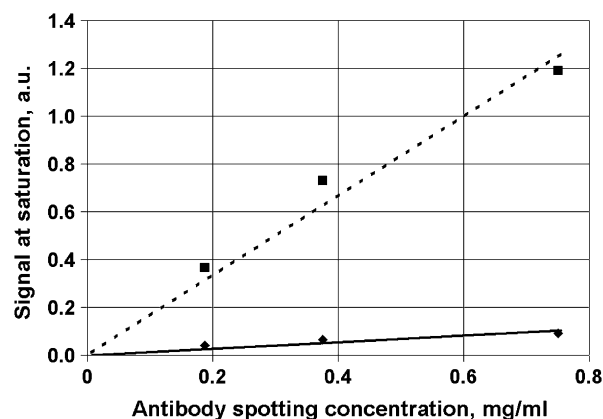


Fig. 5. Dependence of signals at saturation on the concentration of antibodies in spotting solution for the gel-based (■) and surface (◆) protein microchips. Concentration of PSA in analyte solution was 750 ng/ml. The lines (dashed line refers to gel-based microchip, while solid line refers to surface microchip) correspond to the best linear fit of experimental data.

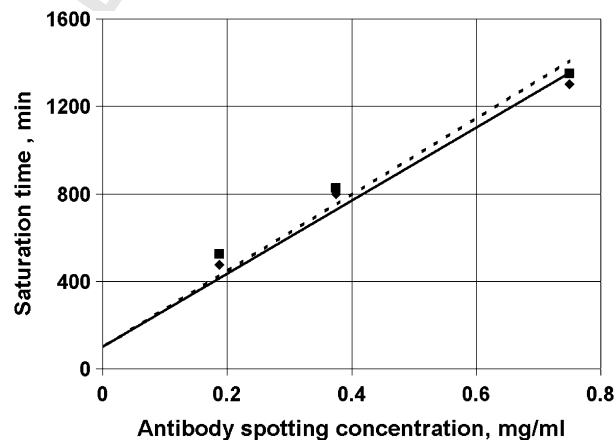


Fig. 6. Dependence of the saturation time on the concentration of antibodies in spotting solution for gel-based (■) and surface (◆) protein microchips. The concentration of PSA in analyte solution was 750 ng/ml. The lines correspond to the best linear fit of experimental data.

binding were similar. Analogous results were also obtained 297  
 at a lower concentration of antigen in buffer solution 298  
 $[Ag]_{sol} = 375 \text{ ng/ml}$  (or  $1.25 \times 10^{-8} \text{ M}$ ). 299

## Discussion 300

### Theoretical overview 301

To interpret the experimental results, we present below 302  
 the relevant theoretical considerations. 303

In the case of direct immunoassay it is assumed that 304  
 fluorescence signals at saturation  $J_{eq}$  detected from the cells 305  
 of both gel-based and surface microchips are proportional 306  
 to the number of complexes  $[C]_{eq}$  formed between antigen 307  
 and immobilized antibodies at the thermodynamic 308  
 equilibrium 309

6

Comparison of surface and gel protein microchips / D.A. Zubtsov et al. / Anal. Biochem. xxx (2007) xxx–xxx

310

$$J_{eq}^{(gel)} = A[C]_{eq} = A[Ab]_{gel} \frac{K_a [Ag]_{sol}}{1 + K_a [Ag]_{sol}} \quad \text{and} \quad (3)$$

$$J_{eq}^{(surf)} = \tilde{A}[\tilde{C}]_{eq} = \tilde{A}[\tilde{Ab}]_{surf} \frac{K_a [Ag]_{sol}}{1 + K_a [Ag]_{sol}}, \quad (4)$$

313 where  $A$  and  $\tilde{A}$  are the apparatus constants for the gel pads  
314 and surface cells, respectively,  $K_a$  is thermodynamic associa-  
315 tion constant (which is equal to the ratio of association  
316 and dissociation rates  $K_a = k_{ass}/k_{diss}$ ),  $[Ag]_{sol}$  denotes the  
317 concentration of the antigen in solution, and  $[Ab]_{gel}$  and  
318  $[\tilde{Ab}]_{surf}$  correspond to the numbers of immobilized anti-  
319 bodies per unit volume of gel pad and per unit area of sur-  
320 face cell.

321 Assuming that the kinetics is diffusion limited, the corre-  
322 sponding characteristic times needed for signal saturation  
323 are defined by  
324

$$\tau_{B,diff}^{(gel)} \cong \frac{R^2}{D_{gel}} [Ab]_{gel} \frac{K_a}{1 + K_a [Ag]_{sol}} \quad \text{and} \quad (5)$$

$$\tau_{B,diff}^{(surf)} \cong \frac{R}{D_{sol}} [\tilde{Ab}]_{surf} \frac{K_a}{1 + K_a [Ag]_{sol}}, \quad (6)$$

327 where  $R$  is the radius of cells and  $D_{gel}$  and  $D_{sol}$  denote the  
328 diffusion coefficients corresponding to the diffusion of anti-  
329 gen in a gel without immobilized antibodies and in analyte  
330 solution. The derivation of Eq. (5) and its experimental jus-  
331 tification can be found in [13]. It has to be noted that if the  
332 external transport is accelerated by mixing devices, the  
333 characteristic diffusion time  $R^2/D_{gel}$  should be replaced  
334 by an effective value dependent on specific conditions of  
335 mixing [14]. The related estimates for the surface kinetics  
336 [Eq. (6)] were obtained in Refs. [15,16].

337 In the case of reaction-limited kinetics the characteristic  
338 binding times are determined as  
339

$$\tau_{B,react} \cong \frac{1}{k_{diss} + k_{ass} [Ag]_{sol}} \quad (7)$$

342 and do not depend on the concentration or density of  
343 immobilized antibodies  $[Ab]_{gel}$  and  $[\tilde{Ab}]_{surf}$ . As the param-  
344 eters  $[Ab]_{gel}$  and  $[\tilde{Ab}]_{surf}$  depend on the concentration of  
345 antibodies  $[Ab]$  in spotting solution, the dependence of  
346 the observable binding times on  $[Ab]$  may serve as the  
347 experimental test for the distinction between alternative re-  
348 gimes of kinetics: if the binding time depends on  $[Ab]$ , the  
349 kinetics is diffusion limited; if it does not, it is reaction  
350 limited.

### 351 Comparison of theoretical predictions with experimental 352 results

353 Now we can use the theoretical predictions for the anal-  
354 ysis of our experimental results.

355 It was implied above that the thermodynamic associa-  
356 tion constants  $K_a$  for the gel-based and surface microchips  
357 are similar. We checked this suggestion by studying the  
358 dependence of fluorescence signals on concentration of  
359 the antigen in solution  $[Ag]_{sol}$  as described by Eqs. (3)–

(6). In particular, we measured the signals at saturation 360  
and the saturation times for two concentrations of antigen 361  
 $[Ag]_{sol} = 750$  ng/ml and  $375$  ng/ml (or  $2.5 \times 10^{-8}$  and 362  
 $1.25 \times 10^{-8}$  M). Based on these data, Eqs. (3)–(6) were used 363  
for the estimation of association constants. The resulting 364  
values were  $K_a = (2.5 \pm 0.3) \times 10^8$  M<sup>-1</sup> for the gel-based 365  
microchips and  $(2.6 \pm 0.2) \times 10^8$  M<sup>-1</sup> for the surface 366  
microchips. The close similarity of association constants 367  
in gel-based and surface protein microchips is in sharp con- 368  
trast with those in oligonucleotide microchips, where steric 369  
restrictions imposed by the immobilization on a flat surface 370  
result in effective suppression of the association constant 371  
on surface chips compared with that on gel chips (see 372  
[15,17] and references therein). 373

374 Thus, the differences in fluorescence signals for both  
375 direct and sandwich immunoassays using gel-based and  
376 surface protein microchips observed in this work cannot  
377 be attributed to the differences in the association con-  
378 stants. In addition, such a suggestion would contradict  
379 the fact that saturation times  $\tau_{B,diff}$  for chips of the  
380 two types are comparable, although the estimated values  
381 of the diffusion coefficient for the gel  $D_{gel}$  are four- to  
382 fivefold lower than the corresponding values measured  
383 in solution  $D_{sol}$  [18].

384 To further clarify the observable features, we assessed  
385 the mean distances between antibodies immobilized in  
386 the gel pads and on the surface cells. The numbers of  
387 immobilized antibodies per unit volume of gel pad  
388  $[Ab]_{gel}$  and per unit area of surface cell  $[\tilde{Ab}]_{surf}$  can be  
389 related to the concentration of antibodies in spotting  
390 solution as 391

$$[Ab]_{gel} = f_i^{(gel)} [Ab]_{spot,sol} \quad \text{and} \quad (8)$$

$$\pi R^2 [\tilde{Ab}]_{surf} = \frac{2\pi}{3} R^3 \cdot f_i^{(surf)} [Ab]_{spot,sol}. \quad (9) \quad 393$$

394 Here  $f_i^{(gel)}$  and  $f_i^{(surf)}$  define the immobilization efficiencies  
395 (or the fractions of immobilized antibodies) for gel pads  
396 and surface cells respectively. Generally, these values  
397 depend on the concentration of antibodies in spotting solu-  
398 tion  $[Ab]_{spot,sol}$  (see Fig. 1). The assessed range of concen-  
399 trations of antibodies immobilized in the gel pads  $[Ab]_{gel}$   
400 was  $2.9 \times 10^{-7} - 4.7 \times 10^{-6}$  M, while the relevant densities  
401 of antibodies immobilized on the surface cells  $[\tilde{Ab}]_{surf}$   
402 amounted to  $1.1 \times 10^{12} - 3.3 \times 10^{12}$  molecules/cm<sup>2</sup>. To  
403 compare these values in comparable units, we calculated  
404 the effective surface density for antibodies immobilized in  
405 the gel pads 406

$$[\tilde{Ab}]_{surf,eff} = R [Ab]_{gel} \quad (10) \quad 408$$

409 obtained by vertical projection of volume concentra-  
410 tions  $[Ab]_{gel}$  in hemispherical gel pads with the radius  $R$   
411 onto their flat base. The relevant densities are reproduced  
412 in Fig. 7 and demonstrate that the effective surface density  
413 for antibodies immobilized in the gel pads can be an order  
414 of magnitude higher than the counterpart density for the  
415 surface antibody microchips.

416 Using the data for the immobilization efficiencies  $f_i$  pre-  
 417 sented in Fig. 2 and Eqs. (8) and (9), the mean distances  
 418 between immobilized antibodies were assessed as

$$d_{gel} = [Ab_i]_{gel}^{-1/3} \quad \text{and} \quad (11)$$

$$420 \quad d_{surf} = [\tilde{Ab}_i]_{surf}^{-1/2}. \quad (12)$$

421 The dependence of these values on the concentration of  
 422 antibodies in spotting solution is shown in Fig. 8. The com-  
 423 parison of Figs. 2 (solid curve) and 8B reveals that the rap-  
 424 id growth in the immobilization efficiency for the surface  
 425 protein microchips begins from the values of  $[Ab]_{spot \ sol}$   
 426 corresponding to  $d_{surf}$  about  $\sim 10$  nm, which is in a good  
 427 accordance with the characteristic molecular sizes of anti-  
 428 bodies determined by X-ray analysis [19] (see also other  
 429 abundant X-ray data in PDB), light scattering [20], and  
 430 atomic force microscopy [21]. The higher and nearly

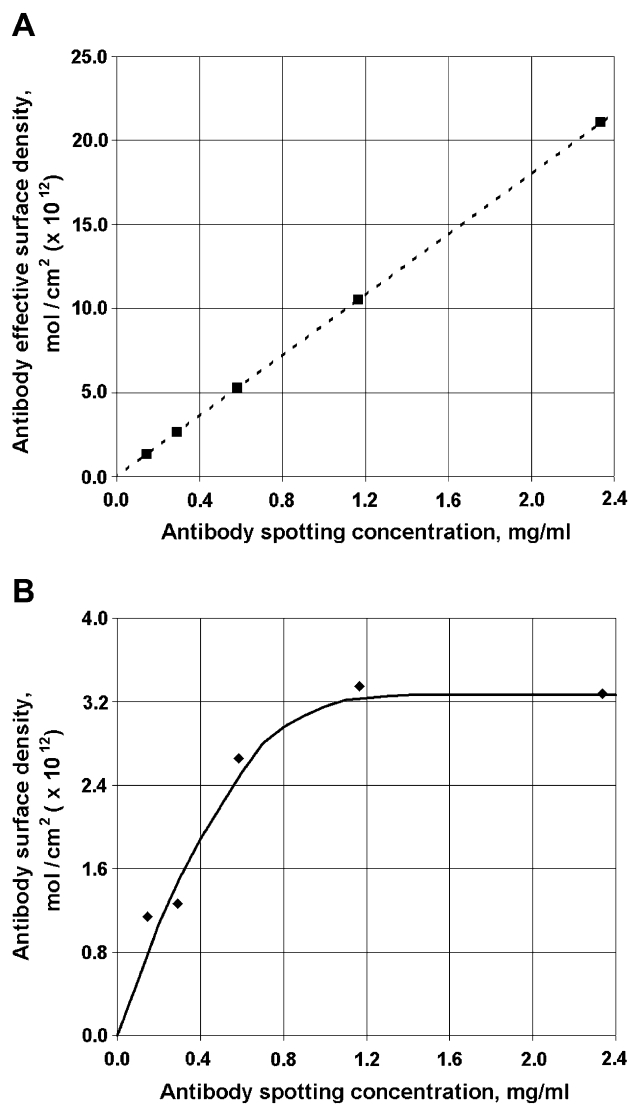


Fig. 7. Comparison of effective surface density for antibodies immobilized in the gel pads (A) [see Eq. (10)] with the corresponding density for antibodies immobilized on the surface cells (B) at different concentrations of antibodies in spotting solution.

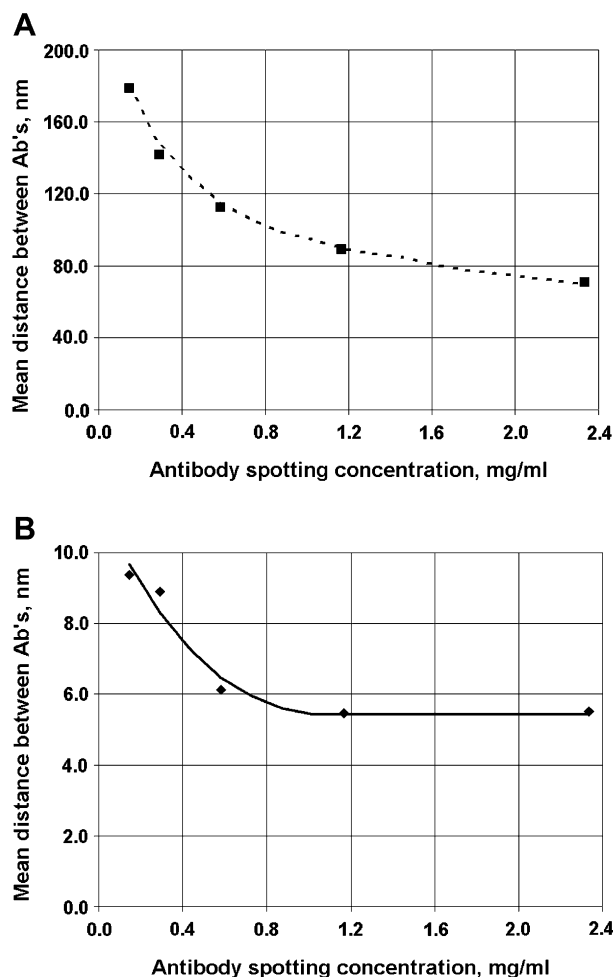


Fig. 8. Dependence of mean distance between immobilized antibodies on the concentration of antibodies in spotting solution for gel-based (A) and surface (B) protein microchips.

constant immobilization efficiency for the gel-based protein 431  
 microchips appears to be concordant with sufficiently large 432  
 mean distances  $d_{gel}$  between antibodies immobilized in the 433  
 gel pads,  $\sim 100$  nm, on the order of magnitude exceeding 434  
 the characteristic molecular sizes of antibodies. 435

The proximity of antibody molecules immobilized on 436  
 the surface cells may hamper their accessibility for the tar- 437  
 get antigen molecules and create steric restrictions for 438  
 molecular antibody-antigen interactions. These effects 439  
 may be approximated in Eqs. (4) and (6) by replacing the 440  
 intensity of fluorescence at saturation and the binding time 441  
 by modified expressions  $J_{eq}^{(surf)} \rightarrow \alpha_{steric} J_{eq}^{(surf)}$  and 442  
 $\tau_{B,diff}^{(surf)} \rightarrow \tau_{B,diff}^{(surf)} / \alpha_{steric}$ , where the factor  $0 < \alpha_{steric} < 1$  reflects 443  
 steric restrictions produced by the close package of anti- 444  
 bodies on the surface cells. This may explain the observable 445  
 difference in the fluorescence signals at the comparable sat- 446  
 uration kinetics in gel-based and surface protein micro- 447  
 chips. These observable features should be partially 448  
 attributed to the random orientation and partial denatur- 449  
 ation for a fraction of antibodies immobilized on a sub- 450  
 strate surface [16]. 451

452 **Conclusion**

453 Our results demonstrate that at the same concentration  
 454 of antibodies in spotting solution gel-based microchips  
 455 provide stronger fluorescence signals than the surface pro-  
 456 tein microchips. The relatively large molecular sizes of anti-  
 457 bodies restrict the maximal density of the probes  
 458 immobilized on the surface cells to  $\sim(3-4) \times 10^{12}$  mole-  
 459 cules/cm<sup>2</sup>, while the capacity of gel pads is much higher.  
 460 Specifically, the concentration of antibodies immobilized  
 461 in gel pads may attain  $10^{-4}$ – $10^{-3}$  M, which is two to three  
 462 orders of magnitude higher than that used in our work.  
 463 The vertical projection of concentrations  $\sim 10^{-4}$ – $10^{-3}$  M  
 464 in hemisphere with the radius 75  $\mu$ m onto its flat base  
 465 would provide the effective surface densities  $\sim 5 \times 10^{14}$ –  
 466  $5 \times 10^{15}$  molecules/cm<sup>2</sup>, never attainable for the surface  
 467 cells (cf. also Fig. 7). However, the limitations connected  
 468 with the rates of binding kinetics impose the condition  
 469  $[Ab]_{gel}K_a \leq 10^3 - 10^4$  and partially restrict the maximal  
 470 capacity of gel pads.

471 Unlike the oligonucleotide microchips [15], the rates of  
 472 signal saturation for the protein microchips of both kinds  
 473 appear to be comparable. The observed saturation times  
 474 for the surface antibody microchips in this work appear  
 475 to be similar to those determined previously by Kusnezov  
 476 et al. [16], while the corresponding times for the gel-based  
 477 antibody microchips are close to values published earlier  
 478 by our group [14].

479 It is worth noting that the diffusion fluxes for the  
 480 hemispherical geometrical body (represented by the gel  
 481 pad) turn out to be more efficient than the diffusion  
 482 fluxes for the flat disk of the same radius and produce  
 483 a more spatially homogeneous distribution of the anti-  
 484 gen–antibody complexes (and, thus, the observable sig-  
 485 nals) than the hemispherical cells in the transient  
 486 regime of binding [22]. If necessary, the binding kinetics  
 487 may be accelerated about fivefold by the active mixing,  
 488 which accelerates the transport of antigen in buffer solu-  
 489 tion [14] (see also [16]).

490 The choice of the optimal platform is one of the  
 491 essential factors in the further development of protein  
 492 microchip technology. The results of this work will be  
 493 useful for the assessment of efficiency of different protein  
 494 microchips.

495 **Acknowledgments**

496 The authors are grateful to E.Ya. Kreidlin for his help in  
 497 microchip manufacturing and all the members of the pro-  
 498 tein biochips group for fruitful discussions. We are also in-  
 499 debted to M.N. Savvateev for his comments on the atomic  
 500 force microscopy methods. We especially thank A.M. Kol-  
 501 chinsky, Health Front Line, Ltd. (Champaign, IL) for his  
 502 assistance in the preparation of this paper and E.I.  
 503 Dementieva for useful remarks. The work was supported  
 504 in part by the Ministry of Science of the Russian  
 505 Federation, State Contract No. 02.190.11.30, code “I-04”.

**References**

- 507 [1] D. Kambhampati (Ed.), Protein Microarray Technology, Wiley–  
 508 VCH Verlag, Weinheim, 2004.  
 509 [2] D. Stoll, J. Bachmann, M.F. Templin, T.O. Joos, Microarray  
 510 technology: an increasing variety of screening tools for proteomic  
 511 research, *Targets* 3 (2004) 24–31.  
 512 [3] C.-S. Chen, H. Zhu, Protein microarrays, *BioTechniques* 40 (2006)  
 513 423–429.  
 514 [4] W. Kusnezow, Y.V. Syagailo, I. Goychuk, J.D. Hoheisel, D.J.  
 515 Wild, Antibody microarrays: the crucial impact of mass transport  
 516 on assay kinetics and sensitivity, *Expert Rev. Mol. Diagn.* 6 (2006)  
 517 111–124.  
 518 [5] A.Yu. Rubina, E.I. Dementieva, A.A. Stomakhin, E.L. Darii, S.V.  
 519 Pan'kov, V.E. Barsky, S.M. Ivanov, E.V. Konovalova, A.D. Mirz-  
 520 abekov, Hydrogel-based protein microchips: manufacturing, prop-  
 521 erties, and applications, *BioTechniques* 34 (2003) 1008–1022.  
 522 [6] A.Yu. Rubina, S.V. Pan'kov, E.I. Dementieva, D.N. Pen'kov, A.V.  
 523 Butygin, V.A. Vasiliskov, A.V. Chudinov, A.L. Mikheikin, V.M.  
 524 Mikhailovich, A.D. Mirzabekov, Hydrogel drop microchips with  
 525 immobilized DNA: properties and methods for large scale produc-  
 526 tion, *Anal. Biochem.* 325 (2004) 92–106.  
 527 [7] E.I. Dementieva, A.Yu. Rubina, E.L. Darii, V.I. Dyukova, A.S.  
 528 Zasedatelev, T.V. Osipova, T.P. Ryabykh, A.Yu. Baryshnikov, A.D.  
 529 Mirzabekov, Protein microchips in quantitative assays for tumor  
 530 markers, *Dokl. Biochem. Biophys.* 395 (2004) 88–92.  
 531 [8] A.Yu. Rubina, V.I. Dyukova, E.I. Dementieva, A.A. Stomakhin,  
 532 V.A. Nesmeyanov, E.V. Grishin, A.S. Zasedatelev, Quantitative  
 533 immunoassay of biotoxins on hydrogel-based protein microchips,  
 534 *Anal. Biochem.* 340 (2005) 317–329.  
 535 [9] T.J. Polascik, J.E. Oesterling, A.W. Parting, Prostate specific antigen:  
 536 a decade of discovery – what we have learned and where we are going,  
 537 *J. Urol.* 162 (1999) 293–306.  
 538 [10] M.J. Barry, Prostate-specific-antigen testing for early diagnosis of  
 539 prostate cancer, *N. Engl. J. Med.* 344 (2001) 1373–1377.  
 540 [11] S.A. Tomlins, M.A. Rubin, A.M. Chinnaiyan, Integrative biology of  
 541 prostate cancer progression, *Annu. Rev. Pathol.: Mechanisms of*  
 542 *Disease* 1 (2006) 243–271.  
 543 [12] V. Barsky, A. Perov, S. Tokalov, A. Chudinov, E. Kreindlin, A.  
 544 Sharonov, E. Kotova, A. Mirzabekov, Fluorescence data analysis on  
 545 gel-based biochips, *J. Biomol. Screen.* 7 (2002) 247–257.  
 546 [13] N.V. Sorokin, V.R. Chechetkin, M.A. Livshits, V.A. Vasiliskov, A.Y.  
 547 Turygin, A.D. Mirzabekov, Kinetics of hybridization on the oligo-  
 548 nucleotide microchips with gel pads, *J. Biomol. Struct. Dyn.* 21 (2003)  
 549 279–288.  
 550 [14] D.A. Zubtsov, S.M. Ivanov, A.Yu. Rubina, E.I. Dementieva, V.R.  
 551 Chechetkin, A.S. Zasedatelev, Effect of mixing on reaction-diffusion  
 552 kinetics for protein hydrogel- based microchips, *J. Biotechnol.* 122  
 553 (2006) 16–27.  
 554 [15] N.V. Sorokin, V.R. Chechetkin, S.V. Pan'kov, O.G. Somova, M.A.  
 555 Livshits, M.Y. Donnikov, A.Y. Turygin, A.S. Zasedatelev, Kinetics  
 556 of hybridization on surface oligonucleotide microchips: theory,  
 557 experiment, and comparison with hybridization on gel-based micro-  
 558 chips, *J. Biomol. Struct. Dyn.* 24 (2006) 57–66.  
 559 [16] W. Kusnezow, Y.V. Syagailo, S. Rüffer, K. Klenin, W. Sebald, J.D.  
 560 Hoheisel, C. Gauer, I. Goychuk, Kinetics of antigen binding to  
 561 antibody microspots: Strong limitation by mass transport to the  
 562 surface, *Proteomics* 6 (2006) 794–803.  
 563 [17] M.S. Shchepinov, S.C. Case-Green, E.M. Southern, Steric factors  
 564 influencing hybridisation of nucleic acids to oligonucleotide arrays,  
 565 *Nucleic. Acids Res.* 25 (1997) 1155–1161.  
 566 [18] A. Pluen, P.A. Netti, R.K. Jain, D.A. Berk, Diffusion of macromol-  
 567 ecules in agarose gels: comparison of linear and globular configura-  
 568 tions, *Biophys. J.* 77 (1999) 542–552.  
 569 [19] E.W. Silvertown, M.A. Navia, D.R. Davies, Three-dimensional struc-  
 570 ture of an intact human immunoglobulin, *Proc. Natl. Acad. Sci. USA*  
 571 74 (1977) 5140–5144.



- 572 [20] R.M. Murphy, H. Slayter, P. Schurtenberger, R.A. Chamberlin, C.K.  
573 Colton, M.L. Yarmush, Size and structure of antigen-antibody  
574 complexes: Electron microscopy and light scattering studies, *Biophys.*  
575 *J.* 54 (1988) 45–56. 578
- 576 [21] N.V. Maluchenko, A.G. Tonevitsky, M.N. Savvateev, V.A. Bykov, S.G. Egorova, M.P. Kirpichnikov, Intermittent-contact atomic force  
577 M.M. Moisenovich, I.I. Agapov, N.V. Kozlovskaya, V.S. Arkhipova, microscopy for investigation of proteins' structural features, *Biofizika*  
48 (2003) 830–836 (in Russian) (English translation: *Biophysics* 48  
[22] P.E. Sheehan, L.J. Whitman, Detection limits for nanoscale biosen- 580  
sors, *Nano Lett.* 5 (2005) 803–807. 581  
582  
583  
584

UNCORRECTED PROOF